PAPER

Composites of ion-in-conjugation polysquaraine and SWCNTs for the detection of H_2S and NH_3 at ppb concentrations

To cite this article: Jin Zhou *et al* 2021 *Nanotechnology* **32** 185502

IOP Publishing Nanotechnology
Nanotechnology 32 (2021) 185502 (10pp) https://doi.org/10.1088/1361-6528/abdf06

Composites of ion-in-conjugation polysquaraine and SWCNTs for the detection of H_2S and NH_3 at ppb concentrations

Jin Zhou[1], Topias Järvinen[1], Olli Pitkänen[1], Zoltán Kónya[2,3], Akos Kukovecz[3,*] and Krisztian Kordas[1,*]

[1] Microelectronics Research Unit, Faculty of Information Technology and Electrical Engineering, University of Oulu, PO Box 4500, FI-90014 Oulu, Finland
[2] MTA-SZTE Reaction Kinetics and Surface Chemistry Research Group of the Hungarian Academy of Sciences, Rerrich Béla tér 1, H-6720 Szeged, Hungary
[3] Interdisciplinary Excellence Centre, Department of Applied and Environmental Chemistry, University of Szeged, Rerrich Béla tér 1, H-6720 Szeged, Hungary

E-mail: kakos@chem.u-szeged.hu and krisztian.kordas@oulu.fi

Received 14 October 2020, revised 12 January 2021
Accepted for publication 22 January 2021
Published 12 February 2021

Abstract

Several different methods are established for the analysis of gases, including optical spectroscopy, photoacoustic spectroscopy as well as colorimetric and resistive sensing, the measurements systems are either too complex or have limited sensitivity. In particular, when the goal is to apply a large number of sensors in networks, it is highly desirable to have devices that are simple, have low cost and energy consumption, yet sensitive and selective to monitor analytes even in traces. Herein, we propose a new type of resistive sensor device based on a composite of single-wall carbon nanotubes and an ion-in-conjugation polymer, poly(1,5-diaminonaphthalene-squaraine), capable of detecting H_2S and NH_3 in air even at room temperature with a theoretical concentration limit of ~1 ppb and ~7 ppb, respectively. Density functional theory calculations revealed that H atoms of the analytes and O atoms of the polymer chain interact and form hydrogen bonds, and the electron withdrawal from the gas molecules by the polymer chain results in the change of its electrical conductivity. To demonstrate the feasibility of the new nanocomposites in sensing, we show the devices for monitoring food safety with good sensor stability of operation for at least 3 months of period of time.

Supplementary material for this article is available online

Keywords: H_2S/NH_3 gas sensors, ion-in-conjugation polymers, polysquaraine, tunneling composites, food quality monitoring

(Some figures may appear in colour only in the online journal)

1. Introduction

H_2S and NH_3 are important reactants of chemical processes. For instance, H_2S is applied in large quantities in oil refinery for catalyst regeneration in hydrodesulfurization, in Kraft paper pulping process, and in mining industry for precipitating metal cations [1]; whereas NH_3 is an indispensable platform chemical used for the production of e.g. nitric acid, fertilizers and organic amines [2]. On the other hand, these gases are also unpleasant concomitants of microbial decomposition of proteins, and are present in sewage systems, biogas and waste management plants, farms, as well as in

* Authors to whom any correspondence should be addressed.

food processing and storage facilities [3–5]. Both gases are corrosive, highly flammable, can irritate the eyes and the respiratory system (at 2 ppm and >30 ppm), can be even lethal (at >500 ppm and >2500 ppm, respectively) [6–12], and their presence in foods (together with organic sulfides and amines) can indicate spoilage. Therefore, detecting and monitoring such analytes have great economic value and play important role in environmental and health safety.

Gas sensors are ubiquitous in health, environmental, transport, infrastructure and industrial safety with continuously growing number of devices due to the expansion of internet-of-things. The ultimate gas sensors are sensitive, selective; and preferably reversible, have long operation life, free of critical elements, and recyclable or at least pose no risk when disposed [13–15]. A large variety of gas sensors exist today including for instance resistive, pellistor, chemical and photogated field-effect transistor, gas ionization device, as well as infrared and photoacoustic spectroscopy based measurement systems among many others [16–20]. Each of these aforementioned technologies has its benefits and disadvantages, however, when it comes to low cost, simplicity, and feasibility to connecting several devices into networks, probably resistive sensors are the most promising candidates among all. Resistive chemical sensing of H_2S and NH_3 has been studied for several materials such as metal oxides [21–23], metal sulfides [24, 25], carbon nanotubes [26, 27] and graphene [28–30]; however, CNTs and graphene based sensors typically lack selectivity and good recovery, whereas metal oxides work at elevated temperatures. Although layered two-dimensional metal sulfide-based sensors hold promise owing to their low temperature operation and high sensitivity, the used transitional metals require proper recovery after the end of life of the devices to maintain long term sustainability and environmental safety.

In the recent years, organic semiconductor materials started to attract research interest in resistive gas sensing due to their large molecular diversity, low cost, good mechanical flexibility, potentially high chemical selectivity and operation at room temperature. Although their versatile chemistry and adjustable microstructure offer great freedoms to tune their intrinsic electrical properties and selective interaction with particular analytes [31–40], only very few materials families have been reported so far. Like for other resistive gas sensors, the sensing performance of organic materials depends largely on the charge transfer from the interaction between analytes and the polymer. The interactions may occur on the surfaces of organic thin films but also in their bulk in case the polymer is porous and/or easily permeable with the gas. The specificity and strength of such noncovalent interactions (hydrogen bonding, π–π stacking and van der Waals forces) determine the variation of carrier density (and indirectly, the type of carrier transport) in the polymer, and thus play critical role in gas sensing [41, 42]. On the one hand, too weak dispersion forces result in poor charge transfer and consequently poor sensitivity and selectivity of the sensor. On the other hand, too strong interactions limit desorption of analytes and can irreversibly alter the chemical structure and electrical properties of the polymer [40, 43, 44]. Therefore, a moderately strong reversible bonding between the gas molecules and sensory materials is critical for good sensing performance. In this regard, squaraines that are resonance-stabilized zwitterionic (N^+ and O^-) structures composed of a squaric ring and an arylamine can offer ideal chemical sensing platforms. Such an ion-in-conjugation structure can form hydrogen bonds but also ion-dipole interactions of medium strength when exposed to target gases [45–47]. Any charge transfer between the gas molecules and the conjugated ion group of squaraine can modulate both the electronic density and shape of the potential well populated by the delocalized electrons thus influencing the local electrical conductivity in nanoscopic volumes of the polymer. However, as the major conduction mechanism in organic semiconductors (and also in squaraine) is charge hopping, the conductivity of the polymers is typically low, and the gas stimulus induced change in the transport is quite limited [38]. To overcome limitations of hopping based carrier transport, a plausible approach is the application of conductive nanomaterial fillers (e.g. metal nanowires, carbon nanotubes, graphene, MXenes) in the polymer host to form composites. Furthermore, the addition of fillers can increase the number of interacting sites with the analytes, increase mobility of charge in organic semiconductor or even enhance the affinity of the composite for gas analytes [44, 48, 49].

Therefore, in this work, we synthesize and explore a new polysquaraine (PDNS, poly(1,5-diaminonaphthalene-squaraine)) and its composites with single-wall carbon nanotubes (SWCNTs) to detect gas analytes at room temperature in chemiresistor-type sensing. The devices based on PDNS-SWCNT composites with optimized composition were able to detect H_2S and NH_3 at a calculated theoretical limit of ~1 ppb and ~7 ppb, respectively, while showing no any response to H_2, CO and CH_4, and only very small to NO. Devices tested for over 3 months proved to have excellent gas response with good repeatability and stability, and were shown to be feasible for monitoring changes of food quality upon storage. Furthermore, we performed simulations to reveal the interaction and charge transfer between the polymer and analytes.

2. Materials and methods

Materials and characterization: Single wall carbon nanotubes (SWCNTs), 1,5-diaminonaphthalene, squaric acid, n-butanol and acetone were ordered from Sigma Aldrich. X-ray photoelectron spectroscopy measurements were performed with a Thermo Fisher Scientific Escalab 250 XI system with an Al Kα source. Raman spectra was performed by Horiba Jobin-Yvon Labram HR800 UV–vis μ-Raman instrument ($\lambda = 448$ nm excitaion). The thermal gravimetric analysis (TGA, Setaram Labsys) was carried out with a 10 °C min^{-1} from room temperature to 800 °C. The microstructure of the synthesized material was studied by field-emission scanning electron microscopy (FESEM, Zeiss ULTRA plus). Infrared spectra were recorded on a Bruker Vertex 70 FT-IR unit in transmission mode. Samples were homogenized in KBr matrix and measured against a pure KBr background.

Synthesis of poly(1,5-diaminonaphthalene-squaraine) (PDNS): 1,5-diaminonaphthalene 790 mg (5 mmol) and

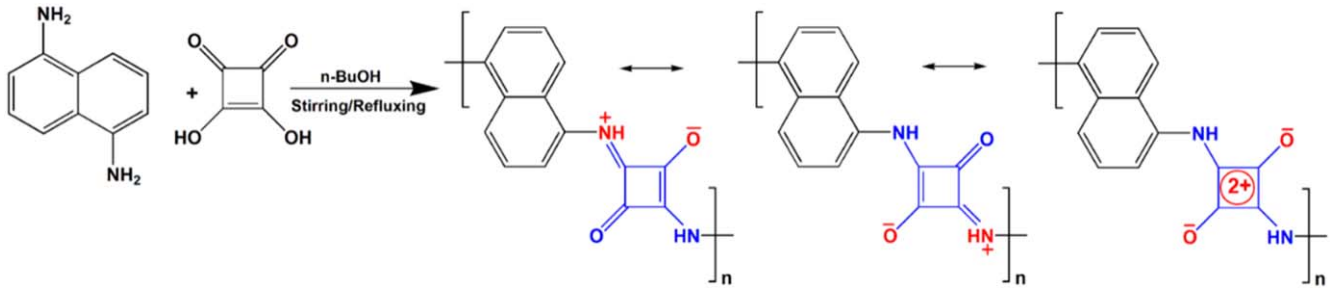

Figure 1. Synthetic route of PDNS, and the scheme of its zwitterionic resonance structure.

squaric acid 570 mg (5 mmol) were dissolved in 35 ml n-butanol in a flask. The mixture was then refluxed and stirred at 120 °C for 16 h. After being cooled to room temperature, the mixture was filtered and washed using acetone and deionized water 10 times. The obtained PDNS was dried in an oven at 80 °C for 24 h. The product was obtained as a dark green powder.

Preparation of PDNS/SWCNT composites: SWCNT and PDNS with mass ratios of 2, 5, 10, 20, 50 and 70 wt% (noted as PDNS-1, PDNS-2, PDNS-3, PDNS-4, PDNS-5 and PDNS-6 respectively) were dispersed in 5 ml ethanol separately using ultrasonication for 1 h and then mixed and stirred for another 1 h at room temperature. Finally, the composite was collected by vacuum filtration.

Sensor preparation and measurements: 20 mg of composite was mixed with 0.5 ml of absolute ethanol to form a paste, which was then brush-coated onto an Al_2O_3 substrate (14 mm × 7 mm) printed with five pairs of Ag–Pd interdigitated electrodes (both electrode distance and width were 200 μm) to form a film, and dried at 70 °C for 2 h. The change of sensor resistance was monitored in a Linkam THMS600 heating and freezing stage connected to an Agilent 3458 A multimeter at 5 V of constant bias. Different concentrations of H_2S, NH_3, NO, CH_4, CO and H_2 were set by LabView driven mass flow controllers. Dry synthetic air (AGA, 20.9% O_2 and 79.1% N_2 at a purity of 5.0) was used as a carrier to dilute these gasses to the desired concentrations and the operating temperature was maintained at near room temperature (30 °C). Exposure periods of 10 min gas pulses, and purging for 30 min between each pulse were applied. The total gas flow rate was set to 500 ml min^{-1} in each experiment. Sensor response is calculated as $(R_g–R_0)/R_0 \times 100\%$, where R_g and R_0 are the resistance of the sensors with and without gas exposure.

Density functional theory calculations (DFT) were performed based on GGA- UBLYP/DNP implemented in DMol3 code. Intermolecular weak interactions were semi-empirically corrected by Tkatchenko–Scheffler scheme [50]. Different adsorption modes were optimized until converging within a criteria of 1×10^{-5} eV in energy and 0.02 eV $Å^{-1}$ in residue force. The Hirshfeld partitioned scheme was applied to analyze charge populations.

3. Results and discussion

3.1. Materials properties

PDNS was synthesized through the condensation between squaric acid (SA) and 1,5-diaminonaphthalene in equimolar ratio in n-butanol under reflux for 16 h [51]. The zwitterionic resonance structure is shown in figure 1.

Fourier-transform infrared spectroscopy of the product and the reactants in figure 2(a) shows the $-NH_2$ and $-OH$ stretches of reactants disappear and new peaks of $-NH-$ stretching emerges in the product indicating the successful reaction of 1,5-diaminonaphthalene and squaric acid, i.e. the formation of PDNS. The characteristic strong absorption peak at 1609 cm^{-1} in PDNS is a result of the zwitterionic resonance of the cyclobutene 1,3-diolate anion moiety. The peak at 1544 cm^{-1} originates from the C=C stretching vibrations of four-membered ring. A small peak at 1791 cm^{-1} is assigned to the ring breathing of the cyclobutene, and the peak at 1703 cm^{-1} means the small amounts 1,2-squarate repeat unit in the polymer chain [52, 53]. Since the intrinsic electrical conductivity of PDNS was found rather small (out of the measurement limit of our setup), we dispersed SWCNTs on the nanoplate shaped PDNS particles (figure 2(b)) with different mass ratios from 2 to 70 wt% and then dispensed the powders onto ceramic chips having printed Ag–Pd interdigital electrodes to form resistive chemical sensor devices (figure 2(c)). According to the FT-IR spectra, the addition of SWCNTs to PDNS does not change the chemical structure.

X-ray photoelectron spectra reveal the N 1s of 1,5-diaminonaphthalene at 398.6 eV, which shifts to ~400 eV and can be resolved with two peaks at 399.8 and 400.2 eV after the reaction with squaric acid indicating the presence of $-NH-$ [54] and $-N^+H=$ [55] groups in the polymer chain, respectively (figure S1(a) (available online at stacks.iop.org/NANO/32/185502/mmedia)). The Raman spectrum of PDNS lacks any peaks i.e. the polymer is amorphous, whereas in the composite we find the characteristic radial breathing mode as well as in-plane (G) and out-of-plane (D) vibration modes of SWCNTs (figure S1(b)). Thermogravimetric analysis (TGA) of the samples indicates high thermal stability of both PDNS and the PDNS/SWCNT composite with an onset of 5% weight loss at 272 °C and 262 °C, respectively (figure S1(c)). The SWCNTs are well

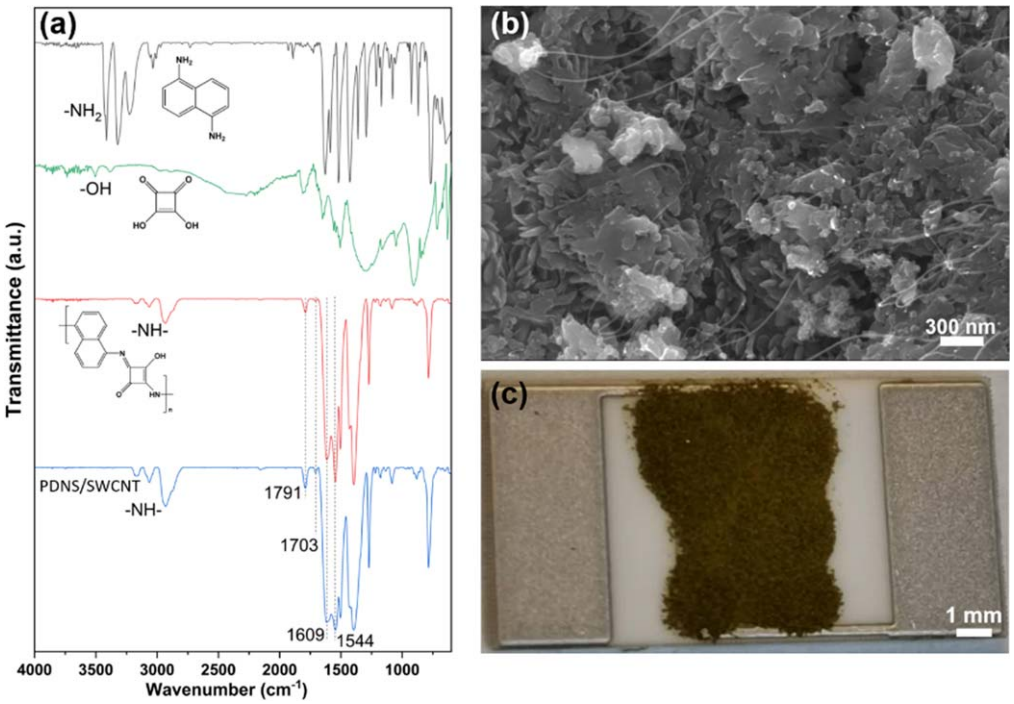

Figure 2. (a) FT-IR spectra of reactants, PDNS and the composite of PDNS/SWCNT. (b) SEM image of the composite and (c) optical picture of the sensor chip with brush coated composite.

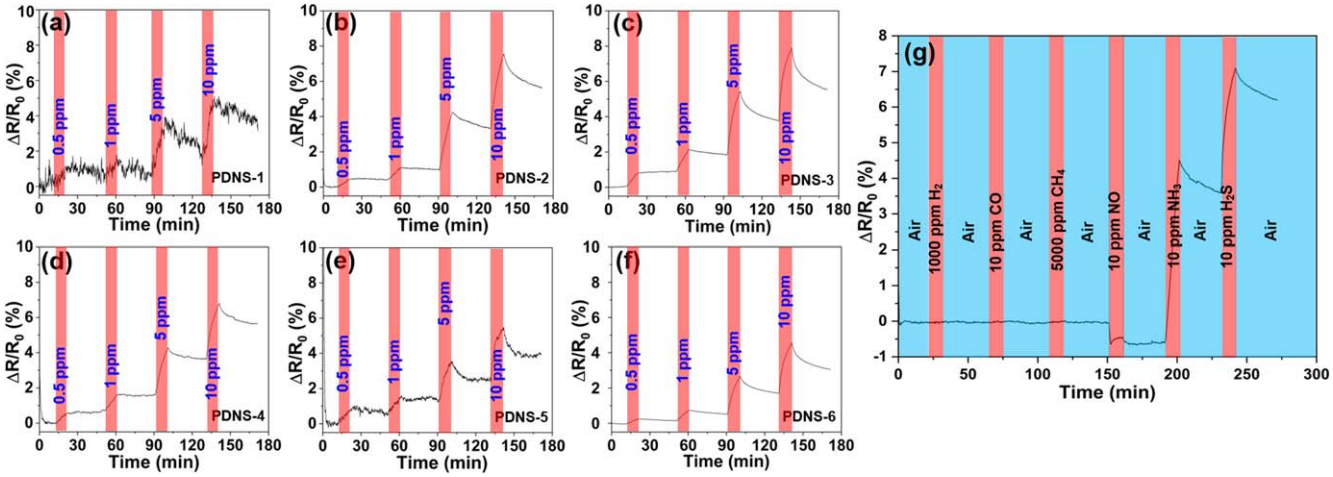

Figure 3. Transient responses curve of sensors based on PDNS-SWCNT composites with SWCNT concentrations of (a) 2 wt%, (b) 5 wt%, (c) 10 wt%, (d) 20 wt%, (e) 50 wt.% and (f) 70 wt% measured for NH_3 at concentrations of 500 ppb, 1 ppm, 5 ppm, and 10 ppm. (g) Gas response of PDNS-3 composite (10 wt% SWCNT) to various analytes in air buffer.

dispersed in the composite as illustrated by scanning and transmission electron micographs shown in figure S2.

3.2. Gas sensing properties

Based on results of preliminary gas exposure experiments, NH_3 was found to induce the highest sensor response, thus we selected this analyte to optimize the composition of the sensing material. Composites of SWCNTs and PDNS with 6 different mass ratios (2, 5, 10, 20, 50 and 70 wt%, noted as PDNS-1, PDNS-2, PDNS-3, PDNS-4, PDNS-5 and PDNS-6) were prepared, and their sensing performance towards NH_3 (from 500 ppb to 10 ppm) buffered in synthetic air were measured. The resistance of composites increases as exposed to NH_3 suggesting p-type semiconducting behavior. The response of sensors shown in figures 3(a)–(f), were found to be the largest for PDNS-3 (1.2 to 2.1-fold compared to other composites with different SWCNT concentrations, as displayed in figure S3) thus we continued our study using the PDNS-3 composite. Screening of sensors to various analytes showed high response for H_2S and NH_3, very moderate for NO, and practically no any for H_2, CO and CH_4. The increased resistance upon exposure to the reducing H_2S with a similar trend to the also reducing NH_3, and decreased resistance on the oxidizing NO gas confirming the p-type semiconducting behavior of the composite (figure 3(g)).

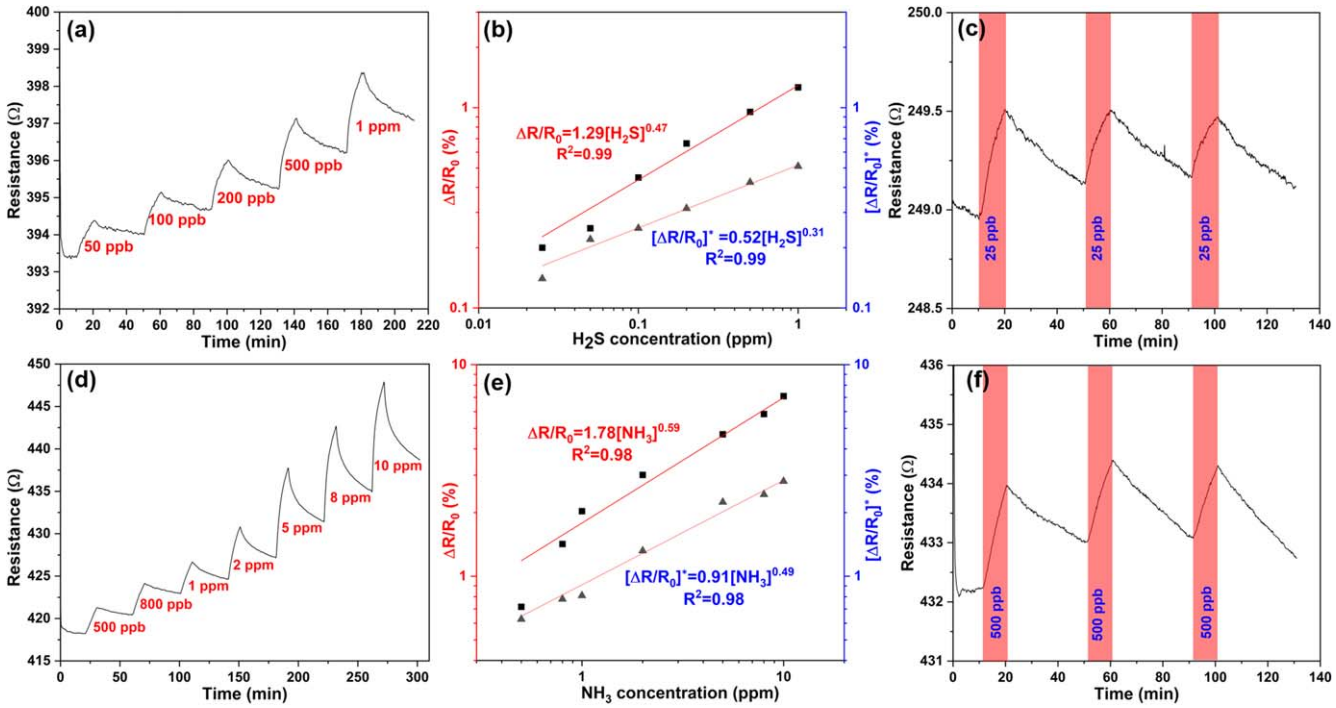

Figure 4. Transient gas response curves of PDNS-3 for the detection of (a) H_2S from 50 ppb to 1 ppm, and (d) NH_3 from 500 ppb to 10 ppm with their corresponding plots of the responses and calibration curves in panels (b) and (e). Repeatability of response curves measured for (c) 25 ppb H_2S and (f) 500 ppb NH_3.

Because of the high response to H_2S and NH_3, we elaborated the measurements using these gases at concentration from 25 ppb to 1 ppm and from 500 ppb and 10 ppm, respectively. The change of sensor resistance upon the gas pulses in air buffer at the applied analyte concentrations (i.e. the $R(c)$ curves) are well defined as shown in figures 4(a) and (d). Based on these $R(c)$ curves, we calculate the responses of the sensors using two methods (figure S4). In the first, we use the initial sensor resistance R_0 to normalize the change of resistance, i.e. $(R_g–R_0)/R_0$, whereas in the other, we consider also the background drift $(R_g–R_0^*)/R_0^*$. Now, by plotting both types of response data for both H_2S and NH_3 as a function of analyte concentrations, we find the obtained calibration curves are nonlinear and follow power functions with fractional exponents similar to those for heterogeneous adsorption (Freundlich model) as displayed in figures 4(b) and (e). Accordingly, the highest sensitivity values appear at low analyte concentrations, and are 1.3% ppm^{-1} for NH_3 and 8.2% ppm^{-1} for H_2S. Experiments with gas mixtures show that analytes inducing small sensor response (H_2, CO or CH_4) are not influencing the response either when introduced in the gas chamber simultaneously with H_2S or NH_3. On the other hand, NO that causes small but opposite sensor response as compared to the other analytes in single analyte experiments, changes the sensor response considerably, when introduced together with H_2S or NH_3. We hypothesize that NO having oxidizing character, reacts with or helps in repelling the adsorbed H_2S or NH_3 from the surface thus *resetting* the sensor. It is also interesting to note that adding a short pulse of 1 ppm NH_3 to a long pulse of 1 ppm H_2S (or vice versa) the responses are superposed on each other (both gases increase resistance in a similar degree), which means that the composite cannot distinguish these two gases from each other (figure S5).

Reproducibility is a critical key performance indicator of gas sensor operation. As shown in figures 4(c) and (f) (and in figures S6 and S7), repeated gas pulses produce nearly identical responses. The slight baseline drift and not entirely complete recovery of the sensors within the time periods (30 min) between subsequent pulses can be improved by increasing the operating temperature (figure S8) or by applying higher flow rates of the flushing gas after the analyte pulses (figure S9) [56]. The noise of the $R(c)$ curves is visibly low, which is due to the improved conductivity of the composite. Consequently, the theoretical limit of detection, which is calculated from the root mean square deviation of base line data and the sensitivity of the sensor (figure S10), as low as 7.4 ppb for NH_3 and 0.8 ppb for H_2S [57]. Such values are lower than those reported for most other sensing materials as listed in the Tables S1 and S2.

To study the effect of operating temperature on the sensing performance, we analyze the response for 1 ppm H_2S and also for 1 ppm NH_3 up to 150 °C [figure 5(a)]. The response of the sensors slightly improves with the increase of the working temperature and after an optimum at 70 °C it decreases. The presence of an optimum operation temperature indicates that several events compete with each other and influence the mechanism of sensing. Usually, increased temperatures cause higher charge transfer efficiency at interfaces, and also help gas molecules diffusing deeper into the bulk of the sensing material [58, 59] thus influencing the sensor response/operation. On the other hand, too high

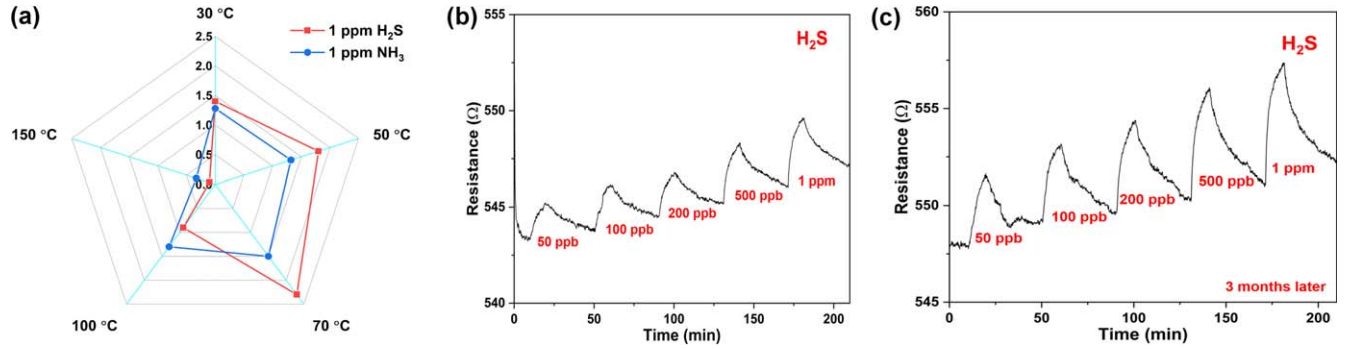

Figure 5. (a) The temperature effect on the sensing response (%). (b) Sensor response for H_2S, and (c) repeated measurement after 3 months of storage in air.

temperatures may compromise adsorption of analytes and interaction of the active sites with those thus reducing the sensitivity [60]. Besides, the recovery of the sensor at 70 °C is better than that at 30 °C and 50 °C, which is reasonable considering the favored analyte desorption process upon flushing with the carrier gas [61]. Furthermore, as shown in figures 5(b) and (c), the sensors have good long term stability measured for over 3 months periods indicating the feasibility of the devices for practical applications.

3.3. Mechanism of sensing

To study the mechanism of sensing with our composite, we assessed the adsorption sites, binding positions and energies of analytes on PDNS (employed by using one repeat unit in PDNS chain) using DFT calculations, and then estimated the degree of the eventual charge by applying the Hirshfeld scheme. Several different adsorption models of H_2S and NH_3 on PDNS chain were surveyed and listed in figures 6(a), (b) and S11. According to the various possible adsorption modes, the ones with hydrogen bonding were showing the largest binding energies with 0.53 eV for H_2S and 0.71 eV for NH_3. Therefore, we may assume that upon exposure of PDNS to H_2S or NH_3, the O and H atoms of the amide in the polymer chain act as active sites, which form double hydrogen bonds with H and S atoms of H_2S (or sulfide) or with N and H atoms of NH_3 (or amine). The moderate adsorption energy of NO (0.34 eV) and the very weak binding with H_2 (0.05 eV), CO (0.12 eV) and with CH_4 (0.07 eV) seem to correlate reasonably well with the observed experimental sensor response to these gases (table 1). It is worth noting here that NO forms a single H-bond, which can also explain the moderate sensor response to this analyte. Furthermore, one may speculate that the Lewis acid/base character of the reactants plays a role in the sensing mechanism viz. both H_2S or NH_3 can be considered as Lewis bases donating their dative electron pairs to the polymer, whereas NO as an acid acts oppositely in qualitative agreement with the sensor response data.

Apart from the intrinsic gas sensing behavior of the polymer, carbon nanotubes present in the composites can also contribute to sensing in several ways. Firstly, CNTs themselves can detect NH_3 [62] and somewhat H_2S [63] and NO [64]. Secondly, in the PDNS-SWCNT composite, the nanotubes can extend the local electric field induced by the adsorbed analytes in the polymer. Thirdly, electrical transport across the tunneling junctions between adjacent SWCNTs in the percolating network may be influenced by the adsorbed moieties on the polymers. In a simplified picture, the tunneling barrier for electrons depends on the position of the LUMO (and for holes on the HOMO) level of the polymer, which shifts upon gas adsorption, consequently changes the tunneling probability. This effect can be significant, since the probability of tunneling [65] through the junction (P) is an exponential function of the barrier height (Φ) as $P = e^{-2d\sqrt{2m\Phi}/\hbar}$, where d is the width of junction and m is the mass of electrons [66–69].

It is important to note here, that SWCNTs added in too high concentration in the composite reduce the gas sensitivity of the sensors (in our case, above 10 wt%), since direct electronic transport is enabled through well-percolated three-dimensional networks of highly conductive metallic nanotubes, which practically shunt the highly resistive tunneling junctions. In such composites, the sensing behavior is limited, and the mechanism is expected to be close to those in pristine and polymer decorated or functionalized CNT networks. To demonstrate the extreme condition, we measure sensing with sensors based on purely SWCNT networks (figure S12), whose gas response is clearly inferior compared to the PDNS-SWCNT composites.

3.4. Sensor application

The freshness of foods with protein content may be monitored by analyzing their decomposition products such as volatile amines and sulfides in the headspace of packaging. Since our sensors have proven to be suitable for detecting NH_3 and H_2S in minute concentrations, we assess whether or not any sensor response would be visible upon measuring the headspace of containers having meat in those (figure S13). Since our sensor material detects both NH_3 and H_2S, which are expected to coexist upon meat degradation, the headspace of the container we apply desiccants to eliminate either of the decomposition products. Namely, to detect NH_3 (and amines) pastilles of NaOH are applied to adsorb and react with H_2S, whereas for the detection of H_2S (and sulfides) powder of P_2O_5 is used to eliminate NH_3. Sensor response data collected for 4 d are compared to the corresponding calibration curves shown in

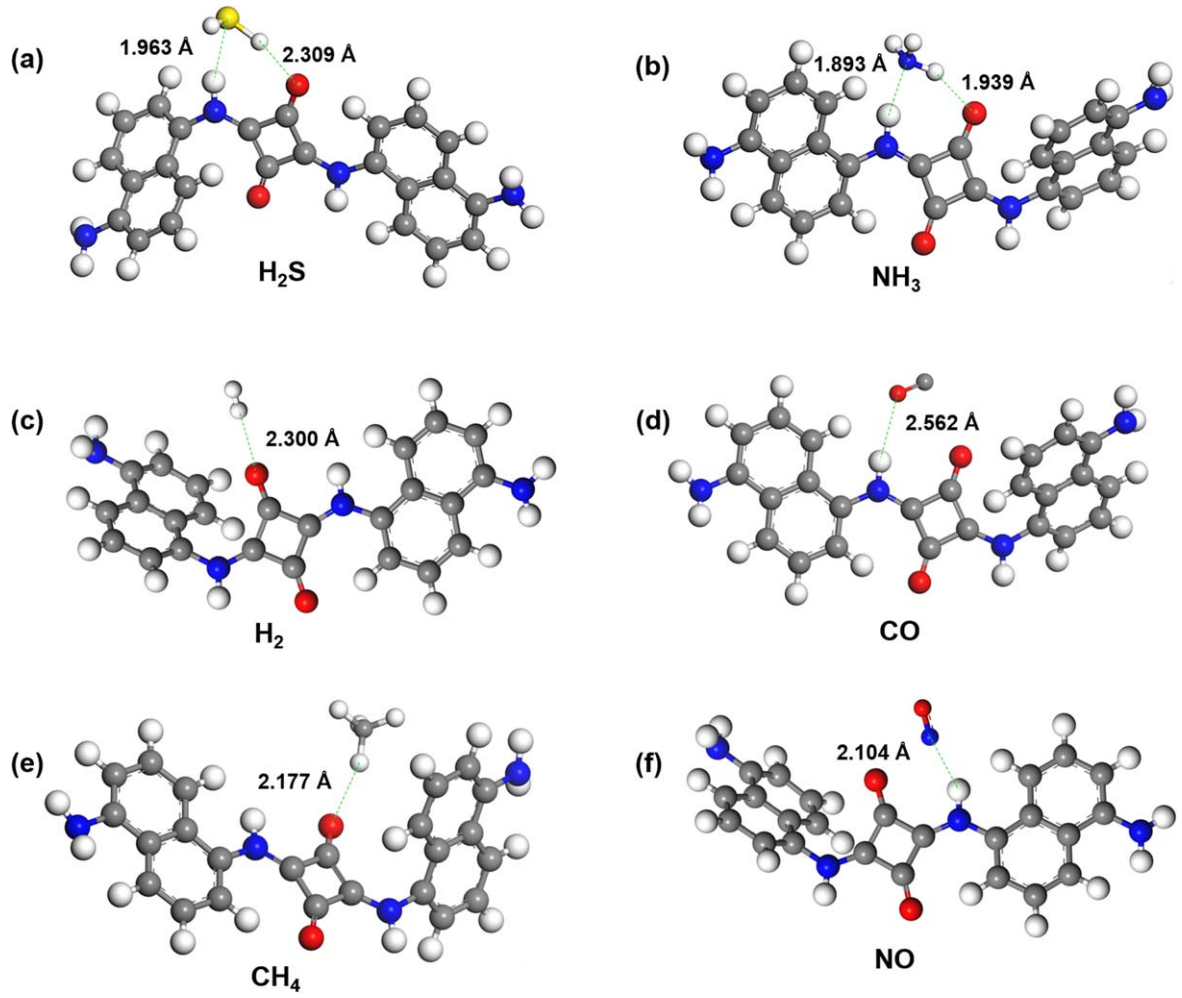

Figure 6. Simulated adsorption of (a) H_2S, (b) NH_3 (c) H_2, (d) CO, (e) CH_4 and (f) NO on PDNS.

Table 1. The bonding length, binding energies and charge transfer of different analytes adsorbed on PDNS.

Analyte	Bonding length (Å)	Binding energy (eV)	Charge transfer (e^-)
H_2S	1.96/2.31	**0.53**	0.03
NH_3	1.89/1.94	**0.71**	0.08
H_2	2.30	0.05	0.05
CO	2.56	0.12	0.02
CH_4	2.18	0.07	0.07
NO	2.10	0.34	0.05

figure 4 to estimate the concentrations of the decomposition products (figure 7). The results suggest that after closing the container, a stabilization period of 12 h is needed, after which the resistance is gradually increasing. After 48 h, the increase of sensor response is pronounced for both types of setups, which indicates that the concentrations of both NH_3 (and amines) and H_2S (and sulfides) have become significantly elevated from 0.8 to 2.2 ppm per gram meat for NH_3, and 2.1–8.3 ppm per gram meat for H_2S. After 4 d, the concentration of NH_3 and H_2S are 70 times and 163 times of that compared to the 0 d, respectively.

4. Conclusions

A new polysquaraine, poly(1,5-diaminonaphthalene-squaraine) was synthesized and compounded with single-wall carbon nanotubes to explore its resistive gas sensing properties. Sensors with optimized polymer to nanotube ratio were found to be highly sensitive H_2S and NH_3 with a theoretical limit of detection of ∼1 ppb and ∼7 ppb, respectively, while showing practically no any response to H_2, CO and CH_4, and only very small to NO. The experimental results are supported well with DFT simulation data suggesting double hydrogen bonding formation between the polymer chain and NH_3 or H_2S. The demonstrated devices showed good stability for at least 3 months of testing period, and proved to be suitable for monitoring the decomposition products of proteins in food packages upon storage.

Our results support previous findings [45–47, 70] on the highly sensitive nature of polysquaraines, and prompts the design of new polymers having ion-in-conjugation structure. Our work also indicates that the addition of conductive fillers (here SWCNTs) can sufficiently improve electrical transport thus making an even poorly condicting polymer a sensing material of practical relevance.

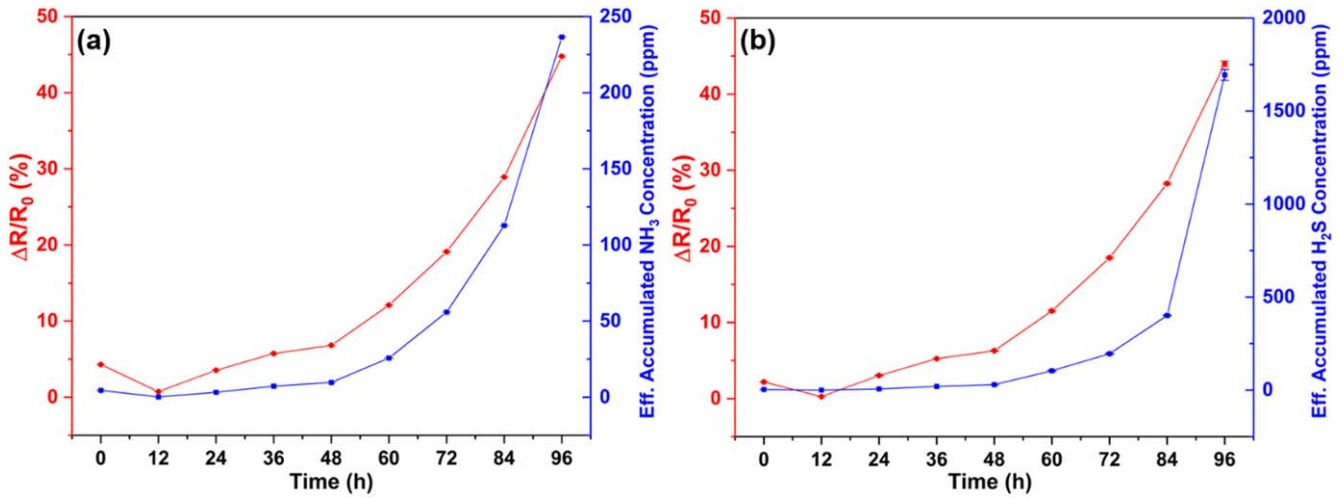

Figure 7. (a) The effective NH_3 and (b) H_2S produced in the storage process of pork at room temperature. The error bars are the standard error of three parallel measurements.

Furthermore, preliminary measurements in gas mixtures show that H_2, CO or CH_4 are not affecting the sensor response to H_2S or NH_3. When NO is added to H_2S or to NH_3 it *resets* the sensor. On the other hand, the response to NH_3 added to H_2S (or other way around) superposes on the other response thus it is not possible to distinguish these two gases in their mixtures. Accordingly, to fully exploit the advantageous sensing propeties of the reported composites, further exploration of sensing in analyte mixtures is needed, and should be combined with systematic data processing e.g. principal and multi-component analyses, pattern recognition and machine learning [71–74].

Acknowledgments

This work was financially supported in part by the University of Oulu (project Entity) and the China Scholarship Council. Financial support by the Hungarian National Research, Development and Innovation Office through projects K126065 and K120115 is acknowledged. We thank the personnel of the Centre for Material Analysis at the University of Oulu for providing us with technical assistance.

Data availability statement

All data that support the findings of this study are included within the article (and any supplementary files).

ORCID iDs

Topias Järvinen https://orcid.org/0000-0002-9256-748X
Olli Pitkänen https://orcid.org/0000-0003-2870-3229
Zoltán Kónya https://orcid.org/0000-0002-9406-8596
Akos Kukovecz https://orcid.org/0000-0003-0716-9557
Krisztian Kordas https://orcid.org/0000-0002-7331-1278

References

[1] Pouliquen F, Blanc C, Arretz E, Labat I, Tournier-Lasserve J, Ladousse A, Nougayrede J, Savin G, Ivaldi R and Nicolas M 2000 Hydrogen sulfide *Ullmann's Encyclopedia of Industrial Chemistry* (Weinheim: Wiley-VCH Verlag GmbH & Co. KGaA) (https://doi.org/10.1002/14356007.a13_467)
[2] Fuhrmann J, Hülsebrock M and Krewer U 2013 Energy storage based on electrochemical conversion of ammonia *Transition to Renewable Energy Systems* ed D Stolen and V Scherer (New York: Wiley) pp 691–706
[3] Zhou X, Lin X, Yang S, Zhu S, Chen X, Dong B, Bai X, Wen X, Geyu L and Song H 2020 Highly dispersed metal-organic-framework-derived Pt nanoparticles on three-dimensional macroporous ZnO for trace-level H_2S sensing *Sensors Actuators* B **309** 127802
[4] Bellare P, Sakhuja N, Kundu S, Bhat N and Ravishankar N 2020 Self-assembled nanostructured tin oxide thin films at the air–water interface for selective H_2S detection *ACS Appl. Nano Mater.* **3** 3730
[5] Ying S, Kong X, Cai Z, Man Z, Xin Y and Liu D 2020 Interactions and microbial variations in a biotrickling filter treating low concentrations of hydrogen sulfide and ammonia *Chemosphere* **255** 126931
[6] Mukhopadhyaya T, Wagner J S, Fan H and Katz H E 2020 Design and synthesis of air-stable p-channel-conjugated polymers for high signal-to-drift nitrogen dioxide and ammonia sensing *ACS Appl. Mater. Interfaces* **12** 21974
[7] Wu J, Wei Y, Ding H, Wu Z, Yang X, Li Z, Huang W, Xie X, Tao K and Wang X 2020 Green synthesis of 3D chemically functionalized graphene hydrogel for high-performance NH_3 and NO_2 detection at room temperature *ACS Appl. Mater. Interfaces* **12** 20623
[8] Yu S H, Cho J, Sim K M, Ha J U and Chung D S 2016 Morphology-driven high-performance polymer transistor-based ammonia gas sensor *ACS Appl. Mater. Interfaces* **8** 6570
[9] Yassine O, Shekhah O, Assen A H, Belmabkhout Y, Salama K N and Eddaoudi M 2016 H_2S sensors: fumarate-based fcu-MOF thin film grown on a capacitive interdigitated electrode *Angew. Chem.* **128** 16111
[10] Li X, Shao C, Lu D, Lu G, Li X and Liu Y 2017 Octahedral-like CuO/In_2O_3 mesocages with double-shell architectures: rational preparation and application in hydrogen sulfide detection *ACS Appl. Mater. Interfaces* **9** 44632

[11] National Research Council (US) Committee on Acute Exposure Guideline Levels 2008 *Acute Exposure Guideline Levels for Selected Airborne Chemicalsa* vol 6 (Washington (DC): National Academies Press (US)) 2, Ammonia Acute Exposure Guideline Levels (https://doi.org/10.17226/12770)

[12] National Research Council (US) Committee on Acute Exposure Guideline Levels 2010 *Acute Exposure Guideline Levels for Selected Airborne Chemicals* vol 9 (Washington (DC): National Academies Press (US)) 4, Hydrogen Sulfide Acute Exposure Guideline Levels (https://doi.org/10.17226/12978)

[13] Kumar R, Al-Dossary O, Kumar G and Umar A 2015 Zinc oxide nanostructures for NO_2 gas-sensor applications: a review *Nano-Micro Lett.* **7** 97

[14] Zhu L and Zeng W 2017 Room-temperature gas sensing of ZnO-based gas sensor: a review *Sensors Actuators* A **267** 242

[15] Jian Y, Hu W, Zhao Z, Cheng P, Haick H, Yao M and Wu W 2020 Gas sensors based on chemi-resistive hybrid functional nanomaterials *Nano-Micro Lett.* **12** 1

[16] Guo J, Wen R, Zhai J and Wang Z L 2019 Enhanced NO_2 gas sensing of a single-layer MoS_2 by photogating and piezo-phototronic effects *Sci. Bull.* **64** 128

[17] Modi A, Koratkar N, Lass E, Wei B Q and Ajayan P M 2003 Miniaturized gas ionization sensors using carbon nanotubes *Nature* **424** 171

[18] Kukkola J *et al* 2012 Inkjet-printed gas sensors: metal decorated WO_3 nanoparticles and their gas sensing properties *J. Mater. Chem.* **22** 17878

[19] Mohl M, Rautio A-R, Asres G A, Wasala M, Patil P D, Talapatra S and Kordas K 2020 2D tungsten chalcogenides: synthesis, properties and applications *Adv. Mater. Interfaces* **7** 2000002

[20] Szakáll M, Huszár H, Bozóki Z and Szabó G 2006 On the pressure dependent sensitivity of a photoacoustic water vapor detector using active laser modulation control *Infrared Phys. Technol.* **48** 192

[21] Dey A 2018 Semiconductor metal oxide gas sensors: a review *Mater. Sci. Eng.* B **229** 206

[22] Zhou Q, Zeng W, Chen W, Xu L, Kumar R and Umar A 2019 High sensitive and low-concentration sulfur dioxide (SO_2) gas sensor application of heterostructure NiO–ZnO nanodisks *Sensors Actuators* B **298** 126870

[23] Fu D, Zhu C, Zhang X, Li C and Chen Y 2016 Two-dimensional net-like SnO_2/ZnO heteronanostructures for high-performance H_2S gas sensor *J. Mater. Chem.* A **4** 1390

[24] Asres G A *et al* 2018 Ultrasensitive H_2S gas sensors based on p-type WS_2 hybrid materials *Nano Res.* **11** 4215

[25] Järvinen T, Lorite G S, Peräntie J, Toth G, Saarakkala S, Virtanen V K and Kordas K 2019 WS_2 and MoS_2 thin film gas sensors with high response to NH_3 in air at low temperature *Nanotechnology* **30** 405501

[26] Wang Y and Yeow J T 2009 A review of carbon nanotubes-based gas sensors *J. Sens.* **2009** 493904

[27] Bahoumina P, Hallil H, Lachaud J-L, Abdelghani A, Frigui K, Bila S, Baillargeat D, Ravichandran A, Coquet P and Paragua C 2017 Microwave flexible gas sensor based on polymer multi wall carbon nanotubes sensitive layer *Sensors Actuators* B **249** 708

[28] Wang C, Lei S, Li X, Guo S, Cui P, Wei X, Liu W and Liu H 2018 A reduced GO-graphene hybrid gas sensor for ultra-low concentration ammonia detection *Sensors* **18** 3147

[29] Park H J, Kim W-J, Lee H-K, Lee D-S, Shin J-H, Jun Y and Yun Y J 2018 Highly flexible, mechanically stable, and sensitive NO_2 gas sensors based on reduced graphene oxide nanofibrous mesh fabric for flexible electronics *Sensors Actuators* B **257** 846

[30] Wang Y, Yang M, Liu W, Dong L, Chen D and Peng C 2019 Gas sensors based on assembled porous graphene multilayer frameworks for DMMP detection *J. Mater. Chem.* C **7** 9248

[31] Jalil A R, Chang H, Bandari V K, Robaschik P, Zhang J, Siles P F, Li G, Bürger D, Grimm D and Liu X 2016 Fully integrated organic nanocrystal diode as high performance room temperature NO_2 sensor *Adv. Mater.* **28** 2971

[32] Han S, Zhuang X, Shi W, Yang X, Li L and Yu J 2016 Poly (3-hexylthiophene)/polystyrene (P3HT/PS) blends based organic field-effect transistor ammonia gas sensor *Sensors Actuators* B **225** 10

[33] Wu X, Mao S, Chen J and Huang J 2018 Strategies for improving the performance of sensors based on organic field-effect transistors *Adv. Mater.* **30** 1705642

[34] Zhuang X, Han S, Huai B, Shi W and Junsheng Y 2019 Sub-ppm and high response organic thin-film transistor NO_2 sensor based on nanofibrillar structured TIPS-pentacene *Sensors Actuators* B **279** 238

[35] Li H, Shi Y, Han G, Liu J, Zhang J, Li C, Liu J, Yi Y, Li T and Gao X 2020 Monolayer two-dimensional molecular crystals for an ultrasensitive OFET-based chemical sensor *Angew. Chem., Int. Ed.* **59** 4380

[36] Lu J, Liu D, Zhou J, Chu Y, Chen Y, Wu X and Huang J 2017 Porous organic field-effect transistors for enhanced chemical sensing performances *Adv. Funct. Mater.* **27** 1700018

[37] Mirza M, Wang J, Wang L, He J and Jiang C 2015 Response enhancement mechanism of NO_2 gas sensing in ultrathin pentacene field-effect transistors *Org. Electron.* **24** 96

[38] Wang Z, Huang L, Zhu X, Zhou X and Chi L 2017 An ultrasensitive organic semiconductor NO_2 sensor based on crystalline TIPS-Pentacene films *Adv. Mater.* **29** 1703192

[39] Wang B, Huynh T P, Wu W, Hayek N, Do T T, Cancilla J C, Torrecilla J S, Nahid M M, Colwell J M and Gazit O M 2016 A highly sensitive diketopyrrolopyrrole-based ambipolar transistor for selective detection and discrimination of xylene isomers *Adv. Mater.* **28** 4012

[40] Low K, Chartuprayoon N, Echeverria C, Li C L, Bosze W, Myung N V and Nam J 2014 Polyaniline/poly(epsilon-caprolactone) composite electrospun nanofiber-based gas sensors: optimization of sensing properties by dopants and doping concentration *Nanotechnology* **25** 115501

[41] Someya T, Dodabalapur A, Huang J, See K C and Katz H E 2010 Chemical and physical sensing by organic field-effect transistors and related devices *Adv. Mater.* **22** 3799

[42] Di C A, Zhang F and Zhu D 2013 Multi-functional integration of organic field-effect transistors (OFETs): advances and perspectives *Adv. Mater.* **25** 313–30

[43] Yang Y, Liang Y, Wang G, Liu L, Yuan C, Yu T, Li Q, Zeng F and Gu G 2015 Enhanced gas-sensing properties of the hierarchical TiO_2 hollow microspheres with exposed high-energy {001} crystal facets *ACS Appl. Mater. Interfaces* **7** 24902

[44] Wang F, Gu H and Swager T M 2008 Carbon nanotube/polythiophene chemiresistive sensors for chemical warfare agents *J. Am. Chem. Soc.* **130** 5392

[45] Yu C, Lin H-Z, Zhou J, Cheng X-F, He J-H, Li H, Xu Q-F, Li N-J, Chen D-Y and Lu J-M 2020 An ion-in-conjugation polymer enables the detection of NO_2 with parts-per-trillion sensitivity and ultrahigh selectivity *J. Mater. Chem.* A **8** 1052

[46] Xiao X, Cheng X F, Hou X, He J H, Xu Q F, Li H, Li N J, Chen D Y and Lu J M 2017 Ion-in-conjugation: squaraine as an ultrasensitive ammonia sensor material *Small* **13** 1602190

[47] Zhou J, Cheng X F, Gao B J, Yu C, He J H, Xu Q F, Li H, Li N J, Chen D Y and Lu J M 2019 Detection of NO_2 down to one ppb using ion-in-conjugation-inspired polymer *Small* **15** 1803896

[48] Srivastava S, Sharma S, Agrawal S, Kumar S, Singh M and Vijay Y 2010 Study of chemiresistor type CNT doped polyaniline gas sensor *Synth. Met.* **160** 529
[49] Abdulla S, Mathew T L and Pullithadathil B 2015 Highly sensitive, room temperature gas sensor based on polyaniline-multiwalled carbon nanotubes (PANI/MWCNTs) nanocomposite for trace-level ammonia detection *Sensors Actuators* B **221** 1523
[50] Tkatchenko A and Scheffler M 2009 Accurate molecular van der Waals interactions from ground-state electron density and free-atom reference data *Phys. Rev. Lett.* **102** 073005
[51] Gauger J and Manecke G 1970 Kondensationsprodukte der Quadratsäure mit primären und sekundären Aminen: II *Chem. Ber.* **103** 3553
[52] Talens V S, Makurat D, Liu T, Dai W, Guibert C, Noteborn W E, Voets I K and Kieltyka R E 2019 Shape modulation of squaramide-based supramolecular polymer nanoparticles *Polym. Chem.* **10** 3146
[53] Chenthamarakshan C and Ajayaghosh A 1998 Synthesis and properties of water-soluble squaraine oligomers containing pendant propanesulfonate moieties *Chem. Mater.* **10** 1657
[54] Neoh K, Kang E and Tan K 1991 Structural dependence of polyanilines on reaction medium *Synth. Met.* **40** 341–54
[55] Tan K, Tan B, Kang E and Neoh K 1991 The chemical nature of the nitrogens in polypyrrole and polyaniline: a comparative study by x-ray photoelectron spectroscopy *J. Chem. Phys.* **94** 5382
[56] Panes-Ruiz L A, Shaygan M, Fu Y, Liu Y, Khavrus V, Oswald S, Gemming T, Baraban L, Bezugly V and Cuniberti G 2018 Toward highly sensitive and energy efficient ammonia gas detection with modified single-walled carbon nanotubes at room temperature *ACS Sens.* **3** 79
[57] Li J, Lu Y, Ye Q, Cinke M, Han J and Meyyappan M 2003 Carbon nanotube sensors for gas and organic vapor detection *Nano Lett.* **3** 929
[58] Al-Hardan N H, Abdullah M J and Abdul Aziz A 2013 Performance of Cr-doped ZnO for acetone sensing *Appl. Surf. Sci.* **270** 480
[59] Li W Q *et al* 2014 Preparation of Pr-doped SnO_2 hollow nanofibers by electrospinning method and their gas sensing properties *J. Alloys Compd.* **605** 80
[60] Assen A Y, Yassine O, Shekhah O, Eddaoudi M and Salama K N 2017 MOFs for the sensitive detection of ammonia: deployment of fcu-MOF thin films as effective chemical capacitive sensors *ACS Sens.* **2** 1294
[61] Cho B, Hahm M G, Choi M, Yoon J, Kim A R, Lee Y-J, Park S-G, Kwon J-D, Kim C S and Song M 2015 Charge-transfer-based gas sensing using atomic-layer MoS_2 *Sci. Rep.* **5** 8052
[62] Kordás K, Mustonen T, Tóth G, Jantunen H, Lajunen M, Soldano C, Talapatra S, Kar S, Vajtai R and Ajayan P M 2006 Inkjet printing of electrically conductive patterns of carbon nanotubes *Small* **2** 1021
[63] Mäklin J, Mustonen T, Halonen N, Tóth G, Kordás K, Vähäkangas J, Moilanen H, Kukovecz Á, Kónya Z and Haspel H 2008 Inkjet printed resistive and chemical-FET carbon nanotube gas sensors *Phys. Status Solidi* b **245** 2335
[64] Mäklin J, Mustonen T, Kordás K, Saukko S, Tóth G and Vähäkangas J 2007 Nitric oxide gas sensors with functionalized carbon nanotubes *Phys. Status Solidi* b **244** 4298
[65] Rahman R and Servati P 2014 Efficient analytical model of conductivity of CNT/polymer composites for wireless gas sensors *IEEE Trans. Nanotechnol.* **14** 118
[66] Maity D and Kumar R T R 2018 Polyaniline anchored MWCNTs on fabric for high performance wearable ammonia sensor *ACS Sens.* **3** 1822
[67] Yoo K-P, Kwon K-H, Min N-K, Lee M J and Lee C J 2009 Effects of O_2 plasma treatment on NH_3 sensing characteristics of multiwall carbon nanotube/polyaniline composite films *Sensors Actuators* B **143** 333
[68] Cho S M, Kim Y J, Kim Y S, Yang Y and Ha S-C 2004 The application of carbon nanotube-polymer composite as gas sensing materials *Sensors, 2004 IEEE,* vol 2 *(Vienna)* p 701
[69] Zhang B, Fu R W, Zhang M Q, Dong X M, Lan P L and Qiu J S 2005 Preparation and characterization of gas-sensitive composites from multi-walled carbon nanotubes/polystyrene *Sensors Actuators* B **109** 323
[70] Zhou J, Lin H, Cheng X-F, Shu J, He J-H, Li H, Xu Q-F, Li N-J, Chen D-Y and Lu J-M 2019 Ultrasensitive and robust organic gas sensors through dual hydrogen bonding *Mater. Horiz.* **6** 554
[71] Kim B, Norman T J, Jones R S, moon D, Han J and Meyyappan M 2019 Carboxylated single-walled carbon nanotube sensors with varying pH for the detection of ammonia and carbon dioxide using an artificial neural network *ACS Appl. Nano Mater.* **2** 6445
[72] Star A, Joshi V, Skarupo S, Thomas D and Gabriel J-C P 2006 Gas sensor array based on metal-decorated carbon nanotubes *J. Phys. Chem.* B **110** 21014
[73] Penza M, Rossi R, Alvisi M and Serra E 2010 Metal-modified and vertically aligned carbon nanotube sensors array for landfill gas monitoring applications *Nanotechnology* **21** 105501
[74] Lentka L, Smulko J M, Ionescu R, Granqvist C G and Kish L B 2015 Determination of gas mixture components using fluctuation enhanced sensing and the Ls-Svm regression algorithm *Metrol. Meas. Syst.* **22** 341